The Influence of Neuromusculoskeletal Model Calibration Method on Predicted Knee Contact Forces during Walking

Gil Serrancolí[*], Allison L. Kinney[#], Benjamin J. Fregly[†], Josep M. Font-Llagunes[*]

[*] Department of Mechanical Engineering
Universitat Politècnica de Catalunya
Av. Diagonal 647, 08028 Barcelona, Catalunya
gil.serrancoli@upc.edu, josep.m.font@upc.edu

[#] Department of Mechanical and Aerospace Engineering
University of Dayton
300 College Park, OH 45469, Dayton, USA
akinney2@udayton.edu

[†] Department of Mechanical and Aerospace Engineering
University of Florida
231 MAE-A Building, FL 32611-6250, Gainesville, USA
fregly@ufl.edu

ABSTRACT

Neuromusculoskeletal models used to predict muscle and joint contact forces for a specific individual require specification of muscle-tendon, skeletal geometry, and neural control model parameter values. Though these parameter values should ideally be calibrated using in vivo data collected from the subject, they are often taken from generic models. This study explored the influence of three model calibration methods on predicted lower limb muscle and knee contact forces during walking. The calibrated model from each approach was used in a static optimization that predicted knee contact forces for six walking trials. The predictions were evaluated using knee contact forces measured *in vivo* from a subject implanted with a force-measuring knee replacement. The first calibration approach used muscle-tendon model parameter values (i.e., optimal muscle fiber lengths and tendon slack lengths) taken directly from the literature. The second approach calibrated muscle-tendon model parameter values such that each muscle operated within a physiological range on the ascending region of its normalized force-length curve. The third approach used a novel two-level optimization that exploited knowledge of the knee contact force measurements to calibrate muscle-tendon, moment arm, and neural control model parameter values such that the calibrated model would predict the *in vivo* contact forces as closely as possible. For the third approach, three walking trials were used to calibrate the model and the remaining three to test the calibrated model. Overall, calibration method had a large affect on predicted knee contact forces. The first method produced highly inaccurate contact force predictions and infeasible solutions for most time frames. The second approach produced accurate medial contact force predictions (average R^2 = 0.89, average RMS error = 107 N) but inaccurate lateral predictions (average R^2 = -1.77, average RMS error = 297 N). The third approach produced accurate testing predictions for both medial (average R^2 = 0.91, average RMS error = 96 N) and lateral (average R^2 = 0.76, average RMS error = 84 N) contact force. These results reveal that when knee contact force data are available, a single set of model parameter values can be successfully calibrated to predict medial and lateral knee contact force accurately over multiple walking cycles. They also reveal that when knee contact force data are not available (the most common situation), a simple calibration method based on muscle operating ranges on their normalized force-length curves may be sufficient to produce accurate medial but not lateral knee contact force predictions.

Keywords: Knee contact forces, muscle force estimation, musculoskeletal model calibration, static optimization, biomechanics

1 INTRODUCTION

The ability to determine muscle and joint contact forces accurately during human movement could be useful for various medical applications, such evaluation of injured subjects at follow-up or prediction of surgical outcome in advance. Experimental measurement of muscle and joint contact forces is not practical in a clinical setting and currently would require invasive

measurement methods (e.g., placing buckle force transducers on tendons). For this reason, numerical methods have been proposed as an alternate means for determining these forces. However, there is indeterminacy in the muscle force calculation process, since the human musculoskeletal system possesses many more muscles than degrees of freedom. Consequently, optimization methods are often applied to solve the indeterminacy problem.

The most common optimization approaches found in the literature are static and dynamic optimization [1,2]. Both are based on the idea that the central nervous system follows a strategy that minimizes some physiological variable (cost function) subject to various constraints. When available, in vivo hip or knee contact force measurements can be used to evaluate lower limb muscle force predictions, although such an approach does not guarantee that the predicted muscle forces will be accurate. Several studies have followed such an approach [3–5]. However, no study has been able to calibrate muscle-tendon, moment arm, and neural control parameter values in a lower limb neuromusculoskeletal model such that the model can predict medial and lateral knee contact forces accurately for multiple walking trials not used in the calibration process. Furthermore, most studies use neuromusculoskeletal model parameter values taken directly from the literature rather than calibrated to the unique functional characteristics of the subject being modeled.

To calibrate parameter values in a neuromusculoskeletal model, researchers should use as much available experimental data as possible to constrain the calibration process. When information is missing, model parameter values should be constrained to remain within physiologically realistic bounds whenever possible. Muscle activations can also be constrained using experimental muscle synergy information [6], potentially reducing the amount of indeterminacy in the muscle force calculation process [5].

The goal of this study was to investigate how predicted leg muscle and knee contact forces differ for three model calibration approaches. Each approach used static optimization applied to a subject-specific musculoskeletal model to estimate muscle forces for six normal walking trials collected from a subject implanted with a force-measuring knee replacement. The first approach used a standard method where all muscle-tendon model parameter values were taken directly from the literature without adjustment or scaling. The second approach pre-calibrated all muscle-tendon model parameter values such that each muscle operated within a physiologically reasonable range on its normalized force-length curve [7,8]. The third approach used a synergy-based two-level optimization formulation that calibrated muscle-tendon as well as moment arm and neural control model parameter values such that static optimization reproduced experimental knee contact force measurements. For all three approaches, three walking trials were used for model calibration and three for testing knee contact force predictions generated by the calibrated model. The results highlight the significant impact that poorly calibrated neuromusculoskeletal model parameter values can have on predicted knee contact and leg muscle forces.

2 METHODS

2.1 Experimental data

Experimental data were taken from the Fourth Grand Challenge Data Competition to Predict In Vivo Knee Loads [4]. Kinematics (marker trajectories and knee fluoroscopy), ground reaction forces/torques, and electromyographic (EMG) data were used from six overground gait cycles (self-selected speed: 1.26 ± 0.03 m/s) of a subject (gender: male, age: 88 years, mass: 65 kg, height: 166 cm) implanted with an instrumented tibial tray. In vivo knee contact force measurements were available for the medial and lateral sides [4]. EMG data were measured for ten lower limb muscles (Adductor Magnus - Addmag; Biceps Femoris Long Head - Bflh; Gastrocnemius Lateralis - GasLat; Gastrocnemius Medialis - GasMed; Peroneus Longus - PerLong; Semimembranosus - Semimem; Soleus - Sol; Tibialis Anterior - TibAnt; Tensor Fascia Latae - TFL; Vastus Lateralis – VasLat). These data were high-pass filtered (fourth-order zero-phase-lag Butterworth filter at 30Hz), rectified, low-pass filtered (fourth-order zero-phase-

lag Butterword filter at 6 Hz) and normalized by the maximum values of all available movement trials. For consistency, knee contact and ground reaction forces were also low-pass filtered (fourth-order zero-phase-lag Butterworth filter at 6 Hz).

2.2 Muscle synergy analysis

Experimental muscle activations were calculated for all six gait trials using an activation dynamics model [9,10]. From these data, a muscle synergy analysis was performed to decompose the activation signals into time-varying neural commands (NCs) (separate for each trial), which represent low-dimensional activation patterns, and corresponding synergy vectors (SVs) (common for all trials), which contain weights defining how each NC contributes to the activation of each muscle [6,11]. A non-negative matrix factorization approach was used to decompose the signals [12]. Muscle synergy information was used in the third calibration approach in an attempt to decrease the amount of indeterminacy in the muscle force calculation process (Section 2.4). To select the number of NCs and SVs (modules) used to parameterize muscle activations for the third calibration approach, we picked the minimum number of modules required to reconstruct activation signals with a variance accounted for higher than 90%, which was five.

2.3 Inverse kinematics and dynamics analyses

A patient-specific musculoskeletal model developed in OpenSim [13] was used to calculate inverse kinematics and dynamics results. The bone geometry of the model was obtained from a CT scan of the subject being modeled [4], while muscle origin and insertion points were defined by scaling a published OpenSim model [14] and then projecting the points to the nearest locations on the subject-specific bone models. The model consisted of the pelvis and the right leg (femur, patella, tibia/fibula, and foot) and possessed 24 degrees of freedom (DOF): 3 rotations and 3 translations between the pelvis and ground, 3 rotations at the hip (flexion, adduction, and rotation), 3 rotations (flexion, adduction, and rotation) and 3 translations (superior-inferior, anterior-posterior. and medial-lateral) at the knee, and 2 rotations (flexion and eversion) at the ankle. Five degrees of freedom (all 3 translations and adduction and internal rotation) of the patella relative to the femur were locked and patellar flexion was constrained to equal knee flexion.

A pose estimation optimization was used to calculate knee kinematics for each walking trial consistent with the knee contact force measurements [15]. Each cost function evaluation involved adjusting the pose parameters (femoral component position and orientation relative to tibial insert) in an elastic foundation (EF) contact model of the subject's tibiofemoral joint. First, an inverse kinematic analysis was performed in OpenSim where all knee DOFs were locked except for the flexion angle. Next, starting from this motion, a pose estimation optimization was used to determine the superior-inferior translation, medial-lateral translation, and adduction rotation in the EF contact model required to match the medial and lateral compressive contact forces measured experimentally and a medial-lateral shear contact force of zero. For each pose estimation optimization, the knee flexion angle was locked to the value predicted by the OpenSim inverse kinematics analysis, while the anterior-posterior translation and internal-external rotation were locked to values measured using fluoroscopy. The kinematics determined from OpenSim and the pose estimation optimization were used in an OpenSim muscle analysis to calculate muscle-tendon lengths, muscle-tendon velocities, and muscle moment arms. Inverse dynamic loads were also calculated in OpenSim using these kinematics plus the experimentally measured ground reactions

2.4 Optimization problem formulation

Static optimization was used to predict leg muscle and knee contact forces for each of the three model calibration approaches evaluated. Approach A used unadjusted literature values for muscle-tendon model parameter values (optimal muscle fiber lengths and tendon slack lengths). Approach B calibrated muscle-tendon model parameter values such that the maximum value of

normalized muscle fiber length over one selected gait cycle was one for each muscle. In these two approaches, moment arms were calculated using the subject-specific OpenSim model (Section 2.3) and experimental muscle activations were not tracked. Approach C used a novel two-level optimization formulation. In the outer level optimization, model parameter values (muscle-tendon plus muscle moment arm and neural control) were adjusted such that the inner level optimization reproduced the experimental knee contact force measurements without knowledge of them. For Approach C, three normal walking trials were used for model calibration purposes and the three remaining trials for testing the calibrated model. The static optimization used to predict leg muscle and knee contact forces was similar for all three approaches. Muscle-tendon units were modeled using a Hill-type musculotendon model possessing a rigid tendon and force-length-velocity properties, where the peak isometric strength of each muscle was set to twice literature values [8]. For each time frame of each gait trial analyzed, six inverse dynamics loads were matched as linear equality constraints: three hip moments (flexion, adduction, and rotation), the knee flexion moment, and two ankle moments (flexion and eversion). These loads were considered to be unaffected by knee contact forces. To ensure that the six inverse dynamic loads could be matched exactly, we included a reserve actuator at each joint with a strength of 0.5 Nm. The cost function minimized the sum of squares of muscle and reserve activations using a quadratic programming algorithm.

The static optimization for Approach C used a slightly different formulation and was the inner level of a two-level optimization method. The Approach C static optimization included additional linear inequality constraints that forced the predicted activations to remain "close" to a linear combination of experimental neural commands. It did not, however, have knowledge of the experimental knee contact force measurements. The outer-level optimization of Approach C adjusted model parameter values such that the inner-level static optimization would predict the correct knee contact forces without knowing them. Design variables for the outer level were the following: scale factors for optimal muscle fiber lengths and tendon slack lengths, moment arm offsets, scale factors for activations of sixteen muscles with associated experimental EMG data, and synergy vector weights for twenty-eight muscles without associated experimental EMG. The cost function for the outer level minimized four sets of terms:

- Tracking terms: Model activations tracked muscle activations reconstructed from experimental neural commands (Section 2.2), while model medial and lateral knee contact forces tracked corresponding experimental forces.
- Bound terms: Model activations and parameter values were constrained within the following bounds: activations reconstructed from experimental neural commands between 0 and 0.7, moment arm offsets between -5 and 5 mm, and scale factors for optimal muscle fiber lengths and tendon slack lengths between ± 20% of literature values [14].
- Constraints: Scale factors for optimal muscle fiber lengths and tendon slack length were constrained to have a maximum deviation of 20%, moment arm offsets and normalized fiber lengths for muscles sharing the same insertion point and exerting a similar function were constrained within 5 mm.
- Minimization terms: Muscle passive forces and reserve activations (from inner-level reserve actuators) were minimized.

Calibration for Approach C involved running the two-level optimization using three walking trials simultaneously in the inner level. At each optimization step, all model parameter values (time invariant) were transferred to the inner level to calculate muscle activations for the three calibration trials (Figure 1). Once all model parameter values were calibrated, testing for Approach C involved running only the inner-level static optimization using the calibrated model parameter values with the three walking trials held back for calibrated model testing purposes.

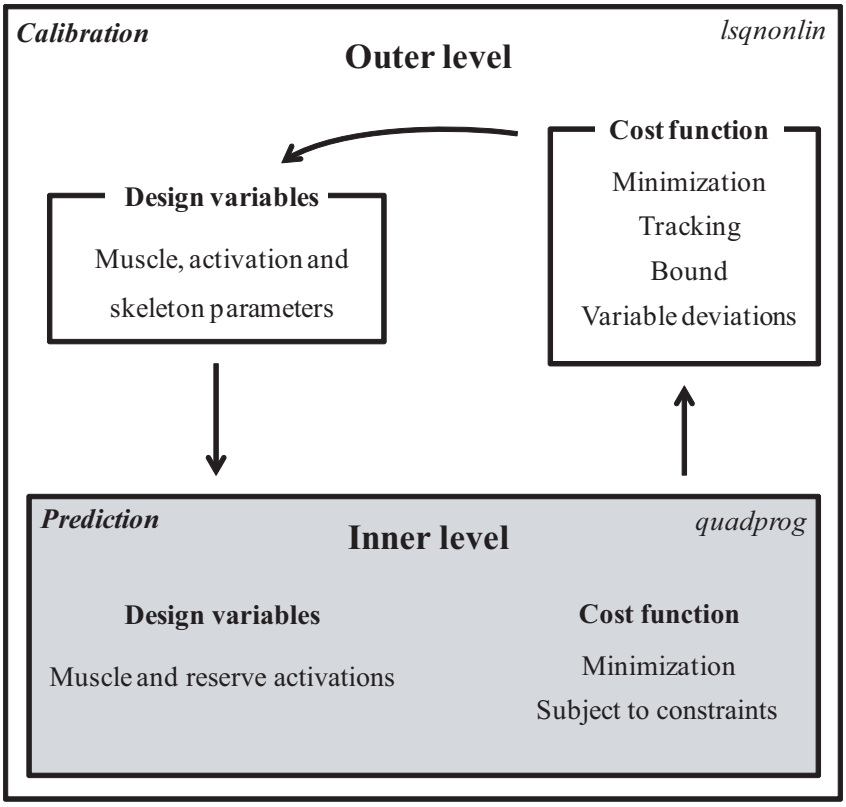

Figure 1. Block diagram of the two-level optimization used in Approach C.

3 RESULTS

3.1 Optimization performance

Musculoskeletal model parameter values (optimal muscle fiber lengths, tendon slack lengths, and moment arms) obtained directly from the literature could not produce realistic muscle activations over all time frames for any of the trials. Therefore, no feasible solutions were reached using Approach A due to excessively high reserve activations (a_{Res} = 1304 ± 2873). Conversely, pre-optimized muscle-tendon model parameter values (Approach B) allowed the static optimization to find reasonable results for all trials using very low values of reserve activations (a_{Res} = 0.000 ± 0.002). Feasible solutions were also found for all trials using Approach C (a_{Res} = 0.04 ± 0.11 for calibration trials and a_{Res} = 0.11 ± 1.2 for prediction trials). For this reason, static optimization outputs were compared only for Approaches B and C in Sections 3.3 and 3.4. The two-level optimization in Approach C required approximately 2 days of CPU time using two 6-core processors Intel Xeon 2.39 GHz processors and 24 GB of RAM. However, the inner-level optimization (i.e., predicting muscle activations in any approach) required just over one second (< 1.2 s) to analyze a complete gait cycle

3.2 Knee contact forces

Without using muscle synergies or calibrated muscle-tendon model parameter values (Approach A), the predicted knee contact forces were unrealistic. Mean medial contact force was 47.4 times larger than the mean experimental value while mean lateral contact force was 36.2 times larger than the corresponding experimental mean. When pre-optimized muscle-tendon model parameter values were used (Approach B), static optimization led to reasonable total contact force magnitudes. For this approach, medial contact force was predicted with reasonable accuracy for all six walking trials ($R^2 > 0.79$, RMSE < 115 N) (Table 1). In contrast, lateral contact force was predicted with poor accuracy, at times (between 25 and 50% of the gait cycle) producing infeasible results where tensile forces would need to be present in the lateral

compartment. When using knee contact force data to calibrate the model (Approach C), highly accurate knee contact force predictions were obtained for all six gait trials (Figure 2 and Table 1). For this approach, accuracy was high not only for the calibration trials (medial RMSE < 121.7 N, lateral RMSE < 112.8 N, total RMSE < 96.7 N) but also for the prediction trials (medial RMSE < 130.1 N, lateral RMSE < 144.3 N, total RMSE < 161.0 N).

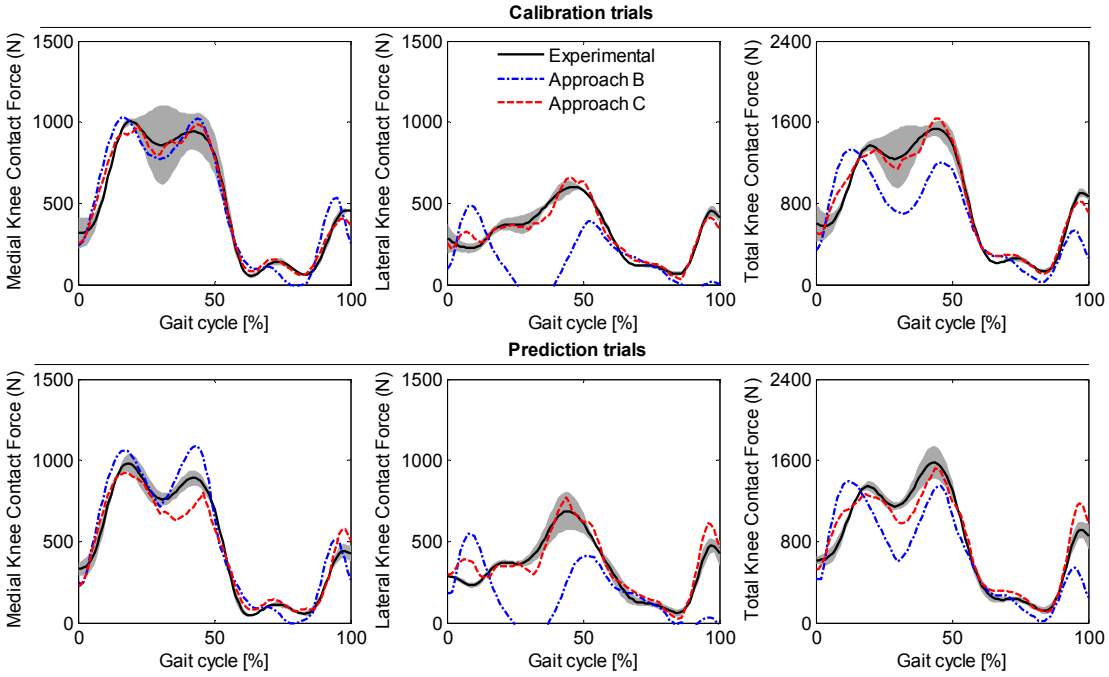

Figure 2. Mean knee contact force predictions. Black solid line represents the mean contact force values of the three gait trials and the grey surface two standard deviations. Dotted blue curves represent the mean values obtained in Approach B and the dashed red curves the mean values obtained in Approach C. Calibration trials were the three gait trials in which the model was calibrated in Approach C and prediction trials were the other three gait trials.

Table 1. Mean and standard deviation of R^2 values (and RMSE) for medial, lateral and total knee contact force predictions for Approaches B and C. Predictions for Approach A were unrealistic.

		Approach B	Approach C
Calibration	Medial	0.91 ± 0.05 (99.5 ± 16.0)	0.97 ± 0.02 (57.0 ± 19.5)
	Lateral	-2.30 ± 1.48 (290.2 ± 67.6)	0.84 ± 0.04 (64.2 ± 7.6)
	Total	0.56 ± 0.09 (323.9 ± 63.5)	0.95 ± 0.01 (110.4 ± 12.6)
Prediction	Medial	0.89 ± 0.08 (107.1 ± 43.0)	0.91 ± 0.03 (96.4 ± 16.7)
	Lateral	-1.77 ± 0.43 (296.5 ± 34.7)	0.76 ± 0.12 (85.4 ± 10.3)
	Total	0.63 ± 0.09 (286.3 ± 9.5)	0.91 ± 0.01 (145.1 ± 15.4)

3.3 Muscle contributions

Variations in muscle forces between Approaches B and C explained the differences in knee contact force predictions. The main difference between these two approaches was that in Approach C, knee contact forces were tracked in the outer level for the calibration trials. Therefore, the differences in total knee varus valgus (VV) muscle moment contributions and superior-inferior (SI) muscle force contributions were different between the two approaches (Figure 3). Individual muscle contributions to these loads were evaluated for the three calibration trials. Differences in VV muscle moment contributions were higher than 1 Nm for four muscles (gaslat, sart, tfl and vaslat). Differences in SI muscle force contributions were

higher than 25 N for five muscles (gaslat, gasmed, sart, tfl and vaslat) (Figure 4). Differences in VV moment during early stance (first 20% of the gait cycle) were primarily due to the fact that vaslat had a much higher VV contribution in Approach B. During the rest of the stance phase, the lower gaslat and tfl VV contributions explained the differences in the total VV moment. The VV peak moment at 95% of the gait cycle in Approach B was due to changes in gaslat and semiten (although the mean semiten moment contribution difference was lower than 1 Nm). During the first 20% of the gait cycle, SI force was higher in Approach B, mainly due to the higher vaslat contribution in Approach B compared to C. For the rest of the cycle, SI muscle force contributions were higher for Approach C, mainly due to higher contributions from gaslat, sart, and tfl. These observed differences between approaches likely relate to difference in calibrated model parameter values.

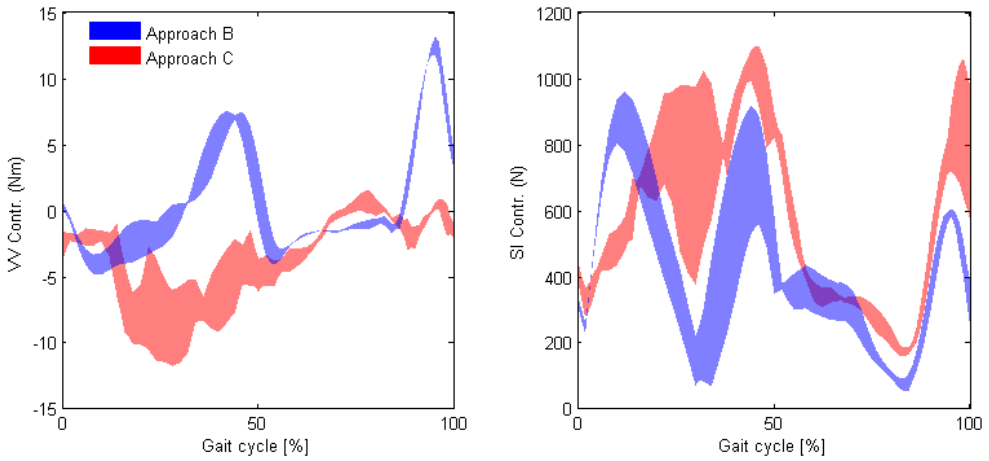

Figure 3. Total knee varus-valgus moment and superior-inferior force contributions between approaches for the three calibration trials.

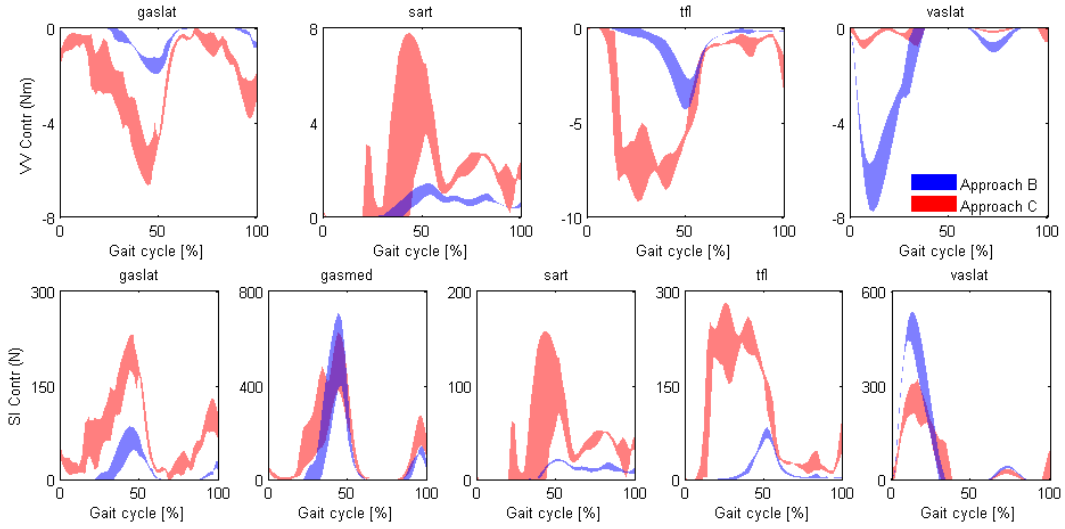

Figure 4. Varus-valgus moment and superior-inferior force contributions for muscles with the greatest differences between approaches for the three calibration trials.

3.4 Model parameter variations

Optimal muscle fiber lengths and tendon slack lengths were higher overall in Approaches B and C compared to Approach A and had high variability (Table 2). For optimal muscle fiber lengths, Approach B values were statistically higher for central muscles and Approach C values higher for medial muscles than in Approach A. For tendon slack lengths, Approach B and C values were statistically higher for all muscles than in Approach A. These differences explain why

Approach A could not find a feasible solution for all time frames. Between Approaches B and C, no statistical differences were observed. The optimal muscle fiber lengths and tendon slack lengths obtained from the literature (Approach A) led to normalized muscle fiber lengths higher than 1.5 for eleven muscles (fdl, fhl, gaslat, gasmed, gem, perbrev, perlong, pertert, piri, soleus, tibpost), representing very high passive muscle force values. For this approach, six of the mentioned muscles had mean passive forces higher than 1000 N, and in three (gasmed, soleus and tibpost) passive forces were higher than 10,000 N, which is unrealistic. For Approaches B and C, all passive forces remained below 200 N. Approach B only had one muscle (soleus) with a mean passive force higher than 20 N, while in Approach C, a mean passive force above 20 N occurred for nine muscles. The higher gaslat passive force would explain the differences in its VV moment and SI force contribution between Approaches B and C observed in Section 3.3.

Given that activation scale factors for Approach C were bounded to be between 0 and 1, these scale factors had high variability (sa = 0.41 ± 0.24 for medial muscles, sa = 0.53 ± 0.64 for central muscles, and sa = 0.38 ± 0.31 for lateral muscles). In Approaches A and B, muscle activations were not tracked, and therefore no activation scale factors were used. The differences in sart and tfl VV moment contributions and SI force contributions between Approaches B and C (Section 3.3) can be explained by changes in muscle activations (Figure A.2, Appendix).

Changes in muscle contributions to inverse dynamics loads also had high variability among muscles. Standard deviation was higher than 1 cm for medial and lateral muscles in the knee flexion moment, for medial muscles in the subtalar moment, and for lateral muscles in the ankle moment. However, only knee superior-inferior offsets for central muscles were statistically different from zero. The differences in vaslat VV moment and gasmed knee SI force contributions (Figure 4) would be explained mainly by their moment arm offsets.

Table 2. Similarity of model parameter values obtained for Approaches B and C relative to Approach A for medial, central, and lateral muscles. Similarities are reported as percent differences for optimal muscle fiber lengths ℓ_o^M and tendon slack lengths ℓ_s^T. Statistically significant differences ($p < 0.05$) in mean values between Approaches B and C relative to Approach A are indicated by a star (*).

	Approach	Medial	Central	Lateral
ℓ_o^M (%)	B	5.0 ± 12.0	10.8 ± 4.9*	6.8 ± 15.5
	C	6.0 ± 13.9*	8.1 ± 13.7	6.0 ± 14.4
ℓ_s^T (%)	B	4.9 ± 12.0*	10.7 ± 4.9*	6.4 ± 15.4*
	C	5.7 ± 14.4*	8.5 ± 6.1*	10.0 ± 12.5*

Table 3. Moment arm offsets obtained in Approach C. Values statistically different from zero are indicated by a star (*). All offsets are reported in mm except for the knee superior-inferior force moment arm, which is dimensionless.

	Medial	**Central**	**Lateral**
Hip flexion	-0.0 ± 6.0	12.3†	-0.0 ± 3.6
Hip adduction	-1.3 ± 6.5	10.14†	2.1 ± 3.5
Hip rotation	0.4 ± 3.3	-1.9†	0.3 ± 7.0
Knee flexion	3.7 ± 11.7	12.7 ± 5.7	3.6 ± 12.4
Knee adduction	-1.3 ± 6.9	4.0 ± 5.3	-2.6 ± 7.3
Knee sup-inf	0.01 ± 0.03	-0.03 ± 0.00*	-0.00 ± 0.01
Subtalar	-1.3 ± 11.1	5.4 ± 7.9	-5.0 ± 6.6
Ankle	-8.4 ± 5.3	-2.4 ± 4.6	-11.1 ± 11.1

†Only one value

4 DISCUSSION

The goals of this study were two-fold. First, we wanted to investigate how model calibration differs when knee contact force data are not used in calibration process (the most common case, Approaches A and B) and when they are used (Approach C). Second, we wanted to evaluate if a set of model parameter values that led to accurate contact force predictions for some walking trials (calibration trials) could predict knee contact forces with comparable accuracy for other walking trials (prediction trials). Approach A used muscle-tendon model parameter values taken directly from the literature [14], whereas in Approach B these parameter values were pre-calibrated. In Approach C, apart from calibrating muscle-tendon model parameter values, we modified skeletal (moment arms) and activation (muscle synergy components) parameter values using a two-level optimization. Using the latter approach, a set of model parameter values was obtained that led to highly accurate knee contact force predictions for the three testing trials. Differences in the predicted knee contact forces and leg muscle forces between the three approaches suggest that poor calibration of neuromusculoskeletal model parameter values may be a primary contributing factor to inaccurate prediction of these internal forces.

While muscle-tendon model parameter values obtained from the literature provide an estimate of the magnitude of these parameter values, they can lead to infeasible static optimization results. For example, Approach A predicted excessively high passive muscle forces. An important finding was that pre-calibrating muscle-tendon model parameter values to make normalized muscle fiber lengths operate on the ascending region of the normalized force-length curve (Approach B) [7], and maintaining these parameter values close to the literature ones, improved knee contact force predictions substantially. In fact, medial contact force predictions for Approach B were surprisingly accurate in terms of both shape and magnitude. However, lateral contact force predictions were still poor, as has been the case in previous studies [16]. The main differences in knee contact predictions between Approach B and Approach C, where neuromusculoskeletal parameter values were calibrated (using knee contact force information in Approach C), can be summarized by changes in five muscles: three lateral muscles (gaslat, tfl, and vaslat) and two medial muscles (gasmed and sart).

Muscle forces obtained in Approaches B and C were similar in magnitude and shape to those predicted in other studies [2,17,18]. Only minor differences were observed for some muscles, such as a lower gmed force in our study compared to in [2]. Nonetheless, overall, all predicted muscle force magnitudes were within the ranges reported in the literature [19].

The main limitation of this study was that all optimizations were carried out using the same movement task, which was overground walking at self-select speed. Using other types of movements, for instance trials were the five muscles mentioned above played a more important role, may lead to a better calibration when no knee contact force data are available (the most usual case) and consequently to better contact force predictions. In addition, only one subject was tested, and trying the three calibration approaches with other subjects would generalize our conclusions. Future research will also explore new ways to introduce more constraints into the static optimization problem formulation.

To conclude, our main recommendation for calculating muscle forces using static optimization is to ensure that muscles operate on the ascending region of their normalized force-length curves. However, such an approach does not ensure that the predicted muscle forces will be correct. We also observed that it was possible to obtain a single set of neuromusculoskeletal model parameter values that predicts accurate knee contact forces for walking trials not used in the calibration process. Further research should be carried out to develop better model calibration methods when no knee contact force data are available.

5 REFERENCES

[1] Erdemir A., McLean S., Herzog W., and Van den Bogert A. J., 2007, "Model-based estimation of muscle forces exerted during movements," Clinical Biomechanics, **22**(2), pp. 131–54.

[2] Anderson F. C., and Pandy M. G., 2001, "Static and dynamic optimization solutions for gait are practically equivalent," Journal of Biomechanics, **34**(2), pp. 153–161.

[3] Stansfield B. W., Nicol a. C., Paul J. P., Kelly I. G., Graichen F., and Bergmann G., 2003, "Direct comparison of calculated hip joint contact forces with those measured using instrumented implants. An evaluation of a three-dimensional mathematical model of the lower limb," Journal of Biomechanics, **36**(7), pp. 929–936.

[4] Fregly B., Besier T., and Lloyd D., 2012, "Grand challenge competition to predict in vivo knee loads," Journal of Orthopaedic Research, **30**(4), pp. 503–513.

[5] Walter J. P., Kinney A. L., Banks S. A., D'Lima D. D., Besier T. F., Lloyd D. G., and Fregly B. J., 2014, "Muscle synergies may improve optimization prediction of knee contact forces during walking.," Journal of Biomechanical Engineering, **136**(2), p. 021031.

[6] Ting L., and Chvatal S., 2010, "Decomposing muscle activity in motor tasks," Motor Control. Theories, Experiments and Applications, p. 19.

[7] Arnold E. M., and Delp S. L., 2011, "Fibre operating lengths of human lower limb muscles during walking.," Philosophical transactions of the Royal Society of London. Series B, Biological sciences, **366**(1570), pp. 1530–1539.

[8] Arnold E. M., Hamner S. R., Seth A., Millard M., and Delp S. L., 2013, "How muscle fiber lengths and velocities affect muscle force generation as humans walk and run at different speeds," The Journal of Experimental Biology, **216**(Pt 11), pp. 2150–2160.

[9] He J., Levine W., and Loeb G., 2002, "Feedback gains for correcting small perturbations to standing posture," Automatic Control, IEEE Transactions on, **36**(3), pp. 322–332.

[10] Winters J., and Stark L., 1988, "Estimated mechanical properties of synergistic muscles involved in movements of a variety of human joints," Journal of Biomechanics, **21**(12), pp. 1027–1041.

[11] Ting L. H., and Macpherson J. M., 2005, "A limited set of muscle synergies for force control during a postural task.," Journal of neurophysiology, **93**(1), pp. 609–613.

[12] Lee D. D., and Seung H. S., 1999, "Learning the parts of objects by non-negative matrix factorization," Nature, **401**, pp. 788–791.

[13] Delp S. L., Anderson F. C., Arnold A. S., Loan P., Habib A., John C. T., Guendelman E., and Thelen D. G., 2007, "OpenSim: open-source software to create and analyze dynamic simulations of movement.," IEEE Transactions on Biomedical Engineering, **54**(11), pp. 1940–50.

[14] Arnold E., Ward S., Lieber R., and Delp S., 2010, "A model of the lower limb for analysis of human movement," Annals of Biomedical Engineering, **38**(2), pp. 269–279.

[15] Bei Y., Fregly B. J., Sawyer W. G., Banks S. A., and Kim N. H., 2004, "The Relationship between Contact Pressure , Insert Thickness , and Mild Wear in Total Knee Replacements," **6**(2), pp. 145–152.

[16] Kinney A., Besier T., D'Lima D., and Fregly B., 2013, "Update on grand challenge competition to predict in vivo knee loads," Journal of Biomechanical Engineering, **135**(2), p. 021012.

[17] Besier T. F., Fredericson M., Gold G. E., Beaupré G. S., and Delp S. L., 2009, "Knee muscle forces during walking and running in patellofemoral pain patients and pain-free controls," Journal of Biomechanics, **42**(7), pp. 898–905.

[18] Fraysse F., Dumas R., Cheze L., and Wang X., 2009, "Comparison of global and joint-to-joint methods for estimating the hip joint load and the muscle forces during walking," Journal of Biomechanics, **42**(14), pp. 2357–2362.

[19] Seth A., and Pandy M. G., 2007, "A neuromusculoskeletal tracking method for estimating individual muscle forces in human movement," Journal of Biomechanics, **40**(2), pp. 356–366.

APPENDIX

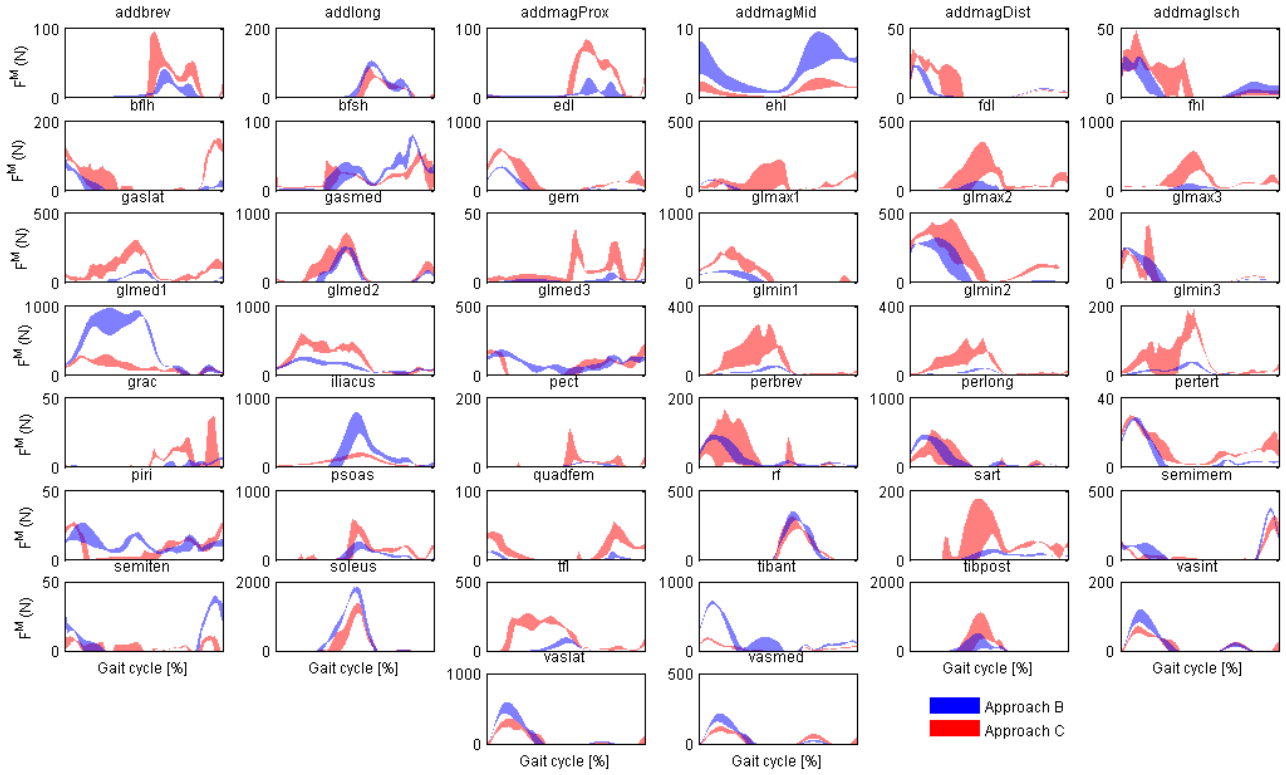

Figure A.1. Muscle forces for all muscles in Approaches B and C.

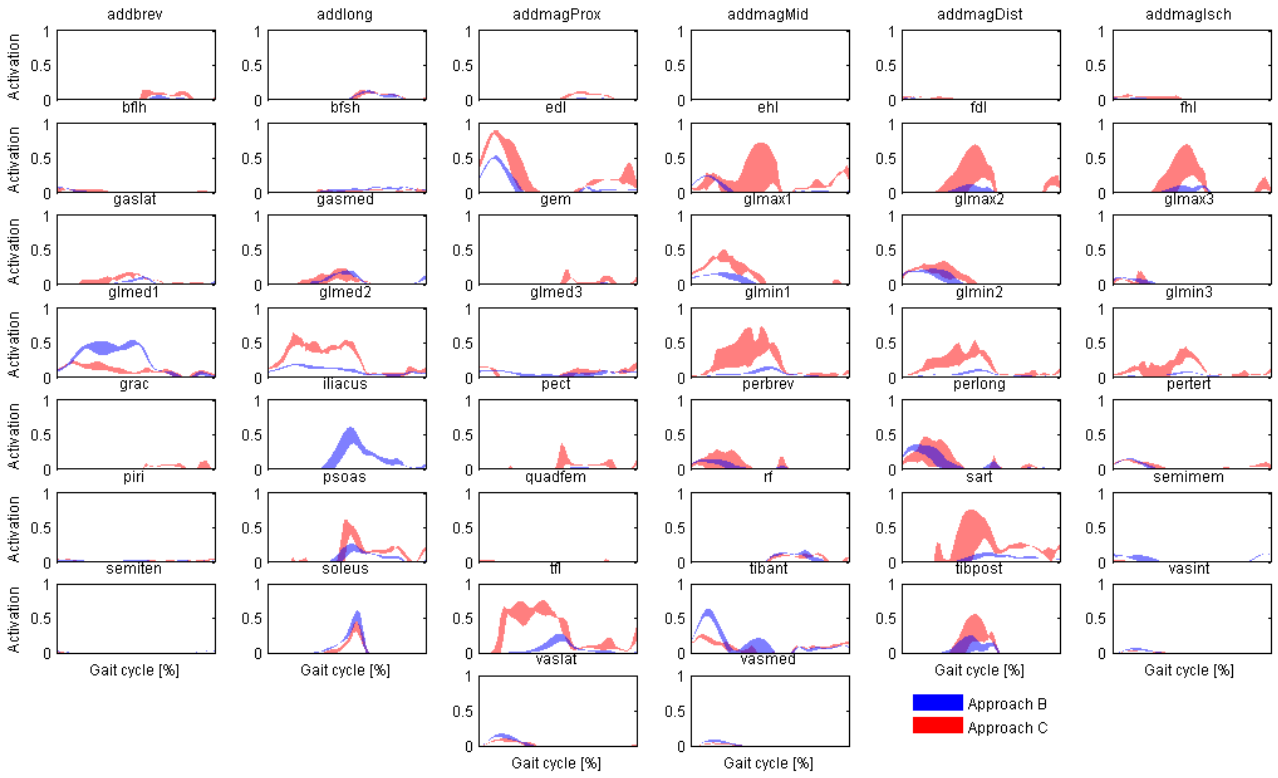

Figure A.2. Muscle activations for all muscles in Approaches B and C.